PAPER Special Section on Multi-dimensional Mobile Information Networks

Error Analysis of Hybrid DS-Multiband-UWB Multiple Access System in the Presence of Narrowband Interference*

Chin-Sean SUM[†a)], Mohammad Azizur RAHMAN[†], *Nonmembers*, Shigenobu SASAKI[††], Hiroshi HARADA[†], *Members*, *and* Shuzo KATO[†], *Fellow*

SUMMARY This paper proposes a hybrid multiband (MB) ultra wideband (UWB) system with direct sequence (DS) spreading. The theoretical error analysis for the DS-MB-UWB multiple access system with Rake receiver in the presence of multipath and narrowband interference is developed. The developed theoretical framework models the multiple access interference (MAI), multipath interference (MI) and narrowband interference for the designed UWB system. It is shown that the system error performance corresponding to the combining effects of these interference can be accurately modeled and calculated. Monte Carlo simulation results are provided to validate the accuracy of the model. Additionally, it is found that narrowband interference can be mitigated effectively in the multiband UWB system by suppressing the particular UWB sub-band co-existing with the interfering narrowband signal. A typical improvement of 5 dB can be achieved with 75% sub-band power suppression. On the other hand, suppression of UWB sub-band is also found to decrease frequency diversity, thus facilitating the increase of MAI. In this paper, the developed model is utilized to determine the parameters that optimize the UWB system performance by minimizing the effective interference.

key words: *error analysis, DS-Multiband-UWB, multiple access interference, multipath interference, narrowband interference, rake receiver*

1. Introduction

The current trend in wireless technology displays increasing emphasis on short-range and high-speed communication systems. Among the overwhelming candidates, ultra wideband (UWB) technology is identified as a possible choice for wireless personal area network (WPAN) [1]. The main encouraging features UWB technology offers are high speed data communication, low complexity low power consumption architectures, the capability to ‘reuse’ the already congested spectrum band in the range of 3.1 to 10.6 GHz [2], and the robustness in multipath environments [3]. One of the popular physical layer design for UWB technology is the orthogonal frequency division modulation (OFDM), which is capable of achieving very high system throughput in a limited bandwidth [4], [5].

Despite of the fact that OFDM-UWB is offering inviting advantages, there are unavoidable tradeoffs. The major setbacks are large system complexity such as high resolution analogue-digital converters (ADC) and expensive power amplifiers, higher dependence on channel coding and interleaving, and higher sensitivity towards frequency synchronization problems. Among the listed disadvantages of OFDM-UWB, system complexity is the most pronounced factor from the perspective of UWB system design. UWB transceivers are supposed to be simple, cost effective and power saving. Employing OFDM systems severely compromises the technical strengths offered by the UWB technology. The analysis of OFDM-UWB will be addressed separately in upcoming investigations and will not be the main focus of this paper.

Therefore, a system design that employs simpler transceiver design is of particular interest. For this purpose, a hybrid multiband (MB) UWB system with DS spreading is proposed in this paper as an alternative design. The DS-MB-UWB system consists of the conventional DS-UWB [6] system with an additional frequency hopping scheme for frequency diversity. In order to analyze the performance of the proposed DS-MB-UWB system, a theoretical framework is developed taking into consideration the impact of multiple access interference (MAI), multipath interference (MI) (commonly known as self interference (SI)), and narrowband interference. The proposed framework is capable of accurately characterizing the system performance corresponding to the combining effects of these interference. Besides, analytical results of the narrowband interference mitigation mechanism in the proposed DS-MB-UWB system can also be obtained.

In existing literatures, we have found most of the UWB error analysis conducted in single band systems. The performance analysis for impulse radio, DS and time hopping (TH) UWB systems are reported in [7]–[10]. The analytical results in hybrid DS-TH-UWB system is reported in [11]. The limitation in these literatures are essentially two fold: Firstly, the literatures mainly focus on additive white Gaussian noise (AWGN) and multiple access channel. Works addressing the combined effects of AWGN, multiple access, and multipath channel in the presence of narrowband interference are not identified so far. Secondly, the literatures have not explored the MB-UWB system, thus overlooked the potentials of frequency diversity.

Therefore, in this paper, we propose the hybrid DS-MB-UWB system and develop its accurate error analysis tool. Our theoretical framework is constructed by applying

Manuscript received December 26, 2008.
Manuscript revised April 1, 2009.
[†]The authors are with National Institute of Information and Communications Technology (NICT), Yokosuka-shi, 239-0847 Japan.
[††]The author is with the Department of Electrical and Electronic Engineering, Niigata University, Niigata-shi, 950-2181 Japan.
*This work was partially presented in IEEE Radio and Wireless Symposium 2008.
a) E-mail: sum@nict.go.jp
DOI: 10.1587/transfun.E92.A.2167

the simplified improved Gaussian approximation (SIGA) framework [12], [13]. We have previously used similar framework and obtained accurate analysis of UWB impulse radio [14], and DS-TH UWB systems [15].

The organization of this paper is as the following. Section 2 presents the DS-MB-UWB signal and system models. Then, Sect. 3 provides the modeling of various types of interference, including MAI, MI and narrowband interference. Next, Sect. 4 discusses the relationship between narrowband interference mitigation and MAI. Section 5 presents the error rate analysis. Section 6 discusses the results based on specific numerical examples. Finally Sect. 7 concludes with potential future works.

2. Signal and System Modeling

We consider a binary phase shift keying (BPSK) DS-MB-UWB system as shown in Fig. 1. The representation of the k-th user's transmitted signal can be given by:

$$s^{(k)}(t) = \sqrt{\frac{E_k}{N_s}} \sum_{i=-\infty}^{\infty} \sum_{j=0}^{N_s-1} d_i c_j^{(k)} p(t - iT_b - jT_c) * \cos[2\pi f_j^{(k)}(t - jT_c)] \quad (1)$$

where d_i is the i-th BPSK data bit uniform over $\{+1, -1\}$, each with bit energy of the k-th user E_k, c_j is the j-th user-dependent DS code of random sequence over $\{+1, -1\}$, N_s is the number of chips per bit, T_b is the bit duration, T_c is the transmitted chip duration, $p(t)$ is the pulse waveform, f_j is the multiband frequency selected randomly from a total of N_B number of sub-bands to form a user-dependent frequency hopping sequence, with probability of each f_j, as $P(f_j) = 1/N_B$, and $P(.)$ denotes the probability.

In (1), the BPSK data is spread by N_s chips each with center frequency f_j. The center frequency is constantly hopping from one sub-band to another, chosen from the total N_B sub-bands. The sub-bands are spectrally orthogonal towards each other. The signaling diagram can be shown in Fig. 2(a) and the spectral diagram in Fig. 2(b). The multiband frequency hopping rate S_r, or how frequent the changing of f_j is, can be expressed by $1/T_c$. In other words, the frequency hopping sequence is assumed to be periodically synchronous with the spreading chip sequence. Each spreading chip from the random spreading sequence is assigned to a distinctive center frequency chosen from the random hopping sequence, as shown in Fig. 2(a).

Here, the sub-band bandwidth W_{sub} is the -10 dB baseband bandwidth of pulse $p(t)$. Hence, W_{sub} and total system bandwidth W_{tot} can be defined as approximately g/T_c [16] and gN_B/T_c respectively, where g is the pulse shape coefficient.

Energy per sub-band E_{sub} can be defined as $E_k P(f_j) = E_k/N_B$. Note that data rate R_b can be given as $1/T_b$. The processing gain (PG) of the system is the ratio of total spreading bandwidth over all sub-bands in use to data rate, given by $N_B W_{sub} T_b$.

Considering a multipath channel with arbitrary fading, the total received signal can be given by:

$$r(t) = \sum_{k=1}^{K} s_r^{(k)}(t - \tau_k) + \eta(t) + \zeta(t) \quad (2)$$

where $s_r^{(k)}(t)$ is the respective received signal from the k-th user, $\eta(t)$ is the AWGN with two sided power spectral density of $N_0/2$ and $\zeta(t)$ represents the narrowband interference. The asynchronism between users can be described as $\tau_k = \alpha_k + \gamma_k T_c$, where τ_k is the random delay of the signal received from user k relative to the desired user (i.e. $\tau_1 = 0$) and τ_k is uniformly distributed over $[0, T_b]$. Here, $0 \leq \alpha_k < T_c$ and γ_k is a random variable (RV) uniform on $\{0, 1, ..., N_s - 1\}$. Additionally, note that $s_r^{(k)}(t)$ is assumed to have a delay spread over multipath channel that generates multipath interference (MI).

Next, the template signal (i.e. the transmitted-signal-equivalent reference signal) for the i-th bit can be described as:

$$s_{tem}^{(1)}(t) = \sum_{j=iN_s}^{(i+1)N_s-1} c_j^{(1)} p_j^{(1)}(t - jT_c) * \cos[2\pi f_j^{(1)}(t - jT_c)] \quad (3)$$

which is placed at multiples of T_c in the multipath channel response for energy capture. This is a path-by-path correla-

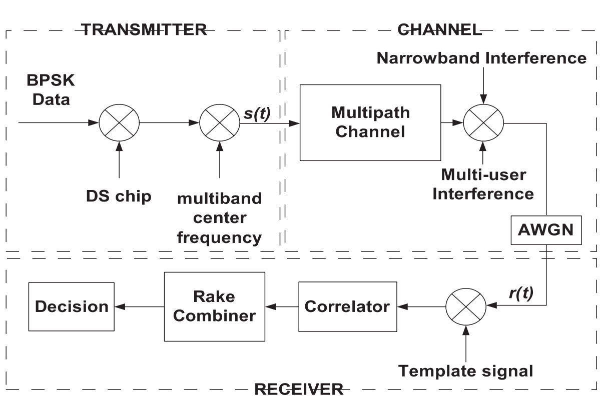

Fig. 1 DS-MB-UWB top level system diagram.

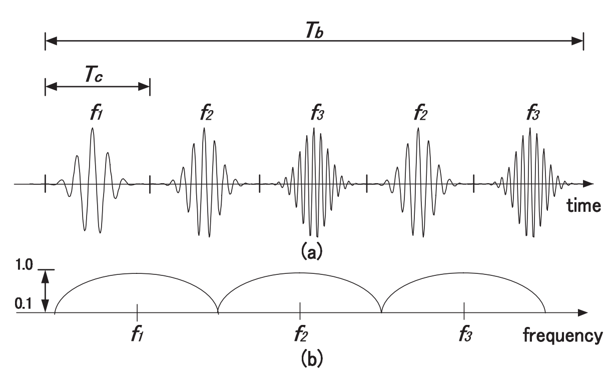

Fig. 2 (a) DS-MB-UWB signaling diagram, (b) Normalized power spectral density of DS-MB-UWB frequency bands (-10 dB bandwidth). In this example: N_s=5,N_B=3.

tor receiver and is equivalent to a matched filter in the frequency domain. We assume that the fading amplitude and phase of the l-th path of the j-th chip of the k-th user at the correlator output to be $\beta_{j,l}^{(k)}$ and $\vartheta_{j,l}^{(k)}$ respectively. Hence, the decision statistics for a coherent correlation receiver while the l-th path of the i-th bit of user 1 is detected can be modeled as:

$$y_l^{(1)} = \sqrt{\frac{E_1}{N_s}} d_i^{(1)} \sum_{j=iN_s}^{(i+1)N_s-1} \beta_{j,l}^{(1)} + \sqrt{\frac{E_1}{N_s}} \sum_{j=iN_s}^{(i+1)N_s-1} U_{j,l} + \sum_{j=iN_s}^{(i+1)N_s-1} \sum_{k=2}^{K} \sqrt{\frac{E_k}{N_s}} V_{j,l}^{(k)} + \sum_{j=iN_s}^{(i+1)N_s-1} S_{j,l} + \eta \tag{4}$$

where the right hand side (RHS) of (4) consists five parts: The first part is the desired signal component. The second part is the MI due to inter chip or symbol interference (ICI/ISI). The third part is the MAI component. The fourth part is the interference generated by the coexisting narrowband signal. The last part is the AWGN component with variance of $\sigma_n^2 = N_0 N_s/2$.

3. Interference Modeling

This section presents the modeling of the interference components as given in (4).

3.1 Multiple Access Interference Modeling

Firstly, we elaborate the model for MAI component $V_{j,l}$ in detail. From the k-th user, the $(j-\gamma_k)$-th and $(j-\gamma_k-1)$-th chips may partially collide with the j-th chip of user 1. However, interference occurs only when the colliding parts belong to the same frequency band $f_j^{(1)}$. We define $\chi_{j-\gamma_k}^{(k)} = [2\pi f_{j-\gamma_k}^{(k)} \alpha_k] \bmod[2\pi]$ and $\chi_{j-\gamma_k-1}^{(k)} = [2\pi f_{j-\gamma_k-1}^{(k)} (T_c - \alpha_k)] \bmod[2\pi]$ that are uniform over $[0, 2\pi]$ to be the phase difference due to asynchronism of the signals. We also assume that the fading phase $\vartheta_{j,l}^{(k)}$ to be uniform over $[0, 2\pi]$. The effect of both χ and ϑ can be modeled by a single variable θ that is uniform over $[0, 2\pi]$. Next, $V_{j,l}^{(k)}$ can be described as:

$$\begin{aligned} V_{j,l}^{(k)} = & \sum_{n=j'-(L-1)}^{j'} P_n^{(k)} \hat{R}_\psi(\alpha_k) \delta(f_n^{(k)}, f_j^{(1)}) \\ & \times \beta_{n,j'-n+1}^{(k)} \cos \theta_{n,j'-n+1}^{(k)} \\ & + \sum_{n=(j'-1)-(L-1)}^{j'-1} Q_n^{(k)} R_\psi(\alpha_k) \delta(f_n^{(k)}, f_j^{(1)}) \\ & \times \beta_{n,j'-n}^{(k)} \cos \theta_{n,j'-n}^{(k)} \end{aligned} \tag{5}$$

where $j' = j + l - 1 - \gamma_k$, L is the total number of paths, $\hat{R}_\psi(\alpha_k)$ and $R_\psi(\alpha_k)$ are continuous-time partial autocorrelation functions of the baseband pulse envelope $p(t)$ defined as $\hat{R}_\psi(\alpha_k) = \int_{\alpha_k}^{T_c} p(t)p(t-\alpha_k)dt$ and $R_\psi(\alpha_k) = \hat{R}_\psi(T_c - \alpha_k)$. The independent RV's $P_n^{(k)}$ and $Q_n^{(k)}$ are uniform on $\{-1, +1\}$, with zero mean and variances $E[(P_n^{(k)})^2] = E[(Q_n^{(k)})^2] = 1$, where n is a counter for ICI from preceding chips hitting on the current instantaneous chip, and $E[.]$ represents mean value. The function of $\delta(f_1, f_2) = 1$, if $f_1 = f_2$; and $\delta(f_1, f_2) = 0$ if otherwise. This is the representation of whether collision takes place between two colliding chips with respective frequency bands.

We employ a Rake type receiver that combines L_c paths ($L_c \le L$) with appropriate weights. Considering W_l being the weight for path l, the decision statistic of (4) after Rake combining becomes $y^{(1)} = \sum_{l=1}^{L_c} W_l y_l^{(1)}$. In a maximal ratio combining (MRC) [17] Rake receiver, the fading amplitude and phase are assumed to be known. In this paper, the multipaths are assumed to be independent of each other.

The next step is to determine the MAI variance $\Psi = \sum_{k=2}^{K} Z_{MAI}^{(k)}$ which is an RV with function of delays $\tau = [\tau_1, \tau_2, ...\tau_K]$. Here, $Z_{MAI}^{(k)} = \sum_{j=iN_s}^{(i+1)N_s-1} Z_j^{(k)}$ where

$$\begin{aligned} Z_j^{(k)} &= \frac{E_k}{N_s} E_{|c} \left[\left(\sum_{l=1}^{L_c} W_l V_{j,l}^{(k)} \right)^2 \right] \\ &= \frac{E_k}{N_s} \sum_{l=1}^{L_c} W_l E_{|c} \left[\left(V_{j,l}^{(k)} \right)^2 \right] \end{aligned} \tag{6}$$

where $E_{|c}[.]$ represents the mean value conditioned on the parameters α_k, $f_j^{(1)}$, $f_n^{(k)}$, $\theta_{j-\gamma_k}^{(k)}$ and $\theta_{j-\gamma_k-1}^{(k)}$

An asynchronous system is considered in the following analysis. The reason of considering only the asynchronous system is that for a practical system with a typical number of tens of users, it is unlikely for the multiple users to have synchronous collisions. Therefore, we dedicate more effort on the analysis of the more realistic asynchronous system. Furthermore, we have previously conducted and reported the analysis on synchronous systems in [15].

Note that interference may only occur if the colliding chips belong to the same frequency band. With α_k as an RV uniformly distributed over $[0, T_c]$, $E_{|c}\left[(V_{j,l}^{(k)})^2\right]$ can be approximated by:

$$\begin{aligned} E_{|c}\left[(V_{j,l}^{k})^2\right] = & \sum_{n=j'-(L-1)}^{j'} \hat{R}_\psi^2(\alpha_k) \delta(f_n^{(k)}, f_j^{(1)}) \\ & \times (\beta_{n,j'-n+1}^{(k)})^2 \cos^2 \theta_{n,j'-n+1}^{(k)} \\ & + \sum_{n=(j'-1)-(L-1)}^{j'-1} R_\psi^2(\alpha_k) \delta(f_n^{(k)}, f_j^{(1)}) \\ & \times (\beta_{n,j'-n}^{(k)})^2 \cos^2 \theta_{n,j'-n}^{(k)} \end{aligned} \tag{7}$$

The probability of colliding signals belonging to the same frequency band is $p = 1/N_B$, and the probability for the signals to be from different frequency bands is $1 - p$. Since the frequency bands of a pulse in any chip pf any user is selected randomly and independently, Thus, the MAI variance for the k-th user, $Z_{MAI}^{(k)}$ can be written as:

$$Z_{MAI}^{(k)} = \frac{E_k}{N_s} \sum_{l=1}^{L_c} W_l^2 \tag{8}$$

$$\left(\sum_{n=l-(L-1)}^{l} X_{n,l}^{(k)} \hat{R}_{\psi}^{2}(\alpha_k)(\beta_{n,((l-n) \mod L)+1}^{(k)})^2 \right.$$
$$\times \cos^2 \theta_{n,((l-n) \mod L)+1}^{(k)}$$
$$\left. + \sum_{n=(l-1)-(L-1)}^{l-1} X_{n,l}^{(k)} R_{\psi}^{2}(\alpha_k)(\beta_{n,l-n}^{(k)})^2 \cos^2 \theta_{n,l-n}^{(k)} \right)$$

where expressions for amplitudes $\beta_{n,((l-n) \mod L)+1}^{(k)}$ and phase $\cos\theta_{n,((l-n) \mod L)+1}^{(k)}$ are taking into consideration the transition between the final part of an instantaneous bit and the beginning of the next bit. Here, X is a RV binomially distributed over $\{0, 1, ..., N_s\}$. Note that X represents the number of chips in a bit of user 1 and the colliding chips of user k belonging to the same band. The probability density function of X can be given as [18]:

$$f_X(x) = \sum_{x=0}^{N_s} \binom{N_s}{x} p^x (1-p)^{N_s - x} \tag{9}$$

with $P(f_j) = p = 1/N_B$ where $\binom{N_s}{x}$ is the binomial coefficient.

3.2 Multipath Interference Modeling

The analysis of MI can be treated as modeling the MAI synchronous system, only that the interference comes from preceding chips of the desired user. By setting $\alpha_k = 0$, we know that $R_\psi(\alpha_k)$=0, $\hat{R}_\psi(\alpha_k)$=1 and $\chi_{j-\gamma_k}$=0. Then, $E_{|c}[(U_{j,l})^2]$ can be described as:

$$E_{|c}\left[(U_{j,l}^{(1)})^2\right] = \sum_{n=j'-(L-1)}^{j'-1} \delta(f_n^{(1)}, f_j^{(1)})(\beta_{n,j'-n+1}^{(1)})^2$$
$$\times \cos^2 \vartheta_{n,j'-n+1}^{(1)} \tag{10}$$

where $E_{|c}[.]$ is the conditional mean value as in (6).

Following similar procedures in modeling MAI, the MI variance can be described as:

$$Z_{MI} = \frac{E_1}{N_s} \sum_{l=1}^{L_c} W_l^2 \sum_{n=l-(L-1)}^{l-1} X_{n,l}^{(1)} (\beta_{n,l-n+1}^{(1)})^2$$
$$\times \cos^2 \vartheta_{n,l-n+1}^{(1)} \tag{11}$$

3.3 Narrowband Interference Modeling

Considering $\Phi(t) = \sqrt{2P_{nrb}}\xi_c(t)\cos(2\pi f_{nrb}t) - \sqrt{2P_{nrb}}\xi_s(t)\sin(2\pi f_{nrb}t)$, as a narrowband signal with center frequency f_{nrb}, signal power P_{nrb}, baseband and RF components ξ_s and ξ_c, to be present within one of the sub-bands, the narrowband interference component $S_{j,i}$ as stated in (4) can be described as:

$$S_{j,l} = \sqrt{2P_{nrb}} B(\epsilon) F(\epsilon) \delta(f_{nrb}, f_j) \tag{12}$$

where ϵ is the phase delay of the narrowband signal relative to the instantaneous chip and is uniform over $[0, 2\pi]$, $B(\epsilon) = \int_{\epsilon}^{T_c} p(t)\xi_s(t-\epsilon)dt$ is the cross-correlation function between the UWB baseband envelope $p(t)$ and the narrowband signal baseband envelope $\xi_s(t)$, and $F(\epsilon)$ is the cross-correlation function between the carrier frequencies of both signals.

Likewise, we can further describe the variance of the narrowband interference as:

$$Z_{nrb} = \sum_{j=iN_s}^{(i+1)N_s-1} E_{|c}\left[\left(\sum_{l=1}^{L_c} W_l S_{j,l}\right)^2\right]$$
$$= 2P_{nrb} \sum_{l=1}^{L_c} Y_l B^2(\epsilon) F^2(\epsilon) \tag{13}$$

where Y_l is an RV binomially distributed over $\{0, 1, ..., N_s\}$ and is the representation of the number of chips in a bit in user 1 that are spectrally overlapping with the narrowband signal center frequency. Also, $E_{|c}[.]$ is the conditional mean value as in (6).

4. Narrowband Interference Mitigation and MAI

From (1) we know that for a frequency hopping sequence with completely random selection of frequency bands, the probability of each sub-band to be selected is equal, $P(f_j) = 1/N_B$, thus distributing the bit energy E_k equally to all sub-bands, each with sub-band energy $E_{sub} = E_k/N_B$.

For interference mitigation purpose, the energy of the particular sub-band affected by the narrowband interference can be suppressed by simply reducing the probability of that sub-band to be selected in the frequency hopping sequence. Thus, the probability of selection of the affected DS-MB-UWB sub-band after suppression can be given as:

$$P(f_{j\_aff}) = \frac{1-\Delta}{N_B} \tag{14}$$

where Δ is the suppression coefficient that determines how much energy is to be suppressed from the sub-band, $0 \leq \Delta \leq 1$ with 0 as no suppression and 1 as full suppression (sub-band elimination). The relationship between Δ and $P(f_{j\_aff})$ can be referred to the solid line in Fig. 3.

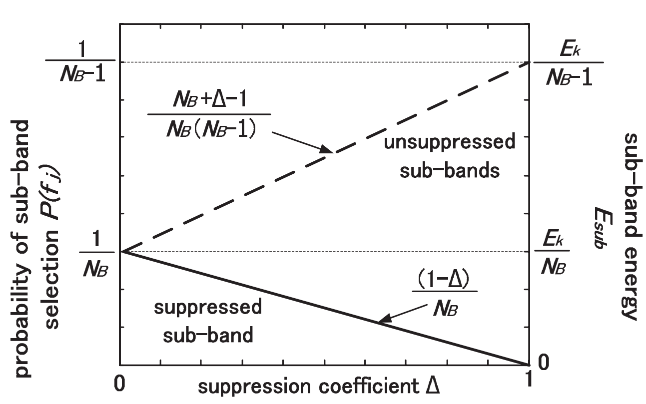

Fig. 3 Relationship between suppression coefficient, sub-band selection probability and sub-band energy.

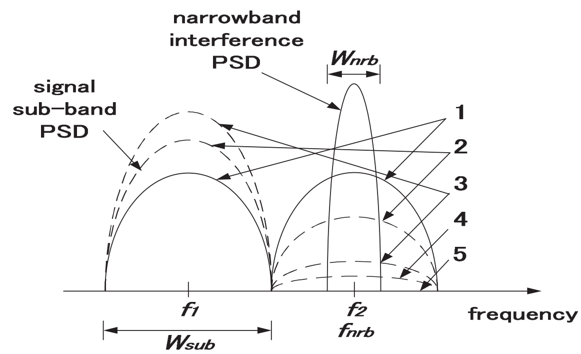

Fig. 4 Spectral diagram of sub-bands with power suppression. Numerical examples of Δ: (1) $\Delta = 0$ (no power suppression), (2) $\Delta = 0.3$, (3) $\Delta = 0.6$, (4) $\Delta = 0.8$, and (5) $\Delta = 1$ (full power suppression).

On the other hand, as the selection probability of the affected sub-band $P(f_{j\_aff})$ is being decreased, other sub-bands unaffected by the narrowband signal will have higher probability of being selected. The probability of each of these 'clean' sub-bands being selected will become:

$$P(f_{j\_clean}) = \frac{N_B + \Delta - 1}{N_B(N_B - 1)} \tag{15}$$

The relationship between Δ and $P(f_{j\_clean})$ can be referred to the dashed line in Fig. 3. Here, note that $P(f_{j\_aff}) \leq P(f_j) \leq P(f_{j\_clean})$. Figure 4 shows the illustration of the sub-band power suppression, ranging from no suppression, partial suppression to band elimination.

By applying sub-band power suppression, the impact of narrowband interference can be mitigated at the expense of decreasing frequency diversity. This is because as larger weights are assigned to select other unaffected sub-bands, the effective hoppable bands become less and thus, decreasing frequency diversity. In other words, by mitigating narrowband interference, MAI and MI are increased due to lower frequency diversity. In order to obtain the best possible performance, a set of optimum combinations of parameters have to be determined. This will be further discussed in the numerical examples.

5. Bit Error Rate

For error analysis of the developed system with interference-detection-mitigation technique, SIGA [12] is employed to calculate the bit error rate (BER) as:

$$\begin{aligned} P_e = &\frac{2}{3}Q\left(\sqrt{\frac{E_1 N_s(\sum_{l=1}^{L_c} W_l\beta_l^{(1)})^2}{\mu_{mai} + \mu_{mi} + \mu_{nrb} + \sigma_n^2 \sum_{l=1}^{L_c} W_l^2}}\right) \\ &+\frac{1}{6}Q\left(\sqrt{\frac{E_1 N_s(\sum_{l=1}^{L_c} W_l\beta_l^{(1)})^2}{\mu_{mai} + \sqrt{3}\sigma_{mai} + \mu_{mi} + \mu_{nrb} + \sigma_n^2 \sum_{l=1}^{L_c} W_l^2}}\right) \\ &+\frac{1}{6}Q\left(\sqrt{\frac{E_1 N_s(\sum_{l=1}^{L_c} W_l\beta_l^{(1)})^2}{\mu_{mai} - \sqrt{3}\sigma_{mai} + \mu_{mi} + \mu_{nrb} + \sigma_n^2 \sum_{l=1}^{L_c} W_l^2}}\right) \end{aligned} \tag{16}$$

where μ_{mai} and σ_{mai} are the mean and standard deviation of the MAI variance Ψ, μ_{mi} is the mean of MI variance Z_{MI}, μ_{nrb} is the mean of narrowband interference variance Z_{nrb}, and $\sigma_n^2 = N_0 N_s/2$ is the AWGN variance. Also, $Q(x) = (2\pi)^{-1/2}\int_x^\infty \exp(-u^2/2)du$. Here, we have assumed that the channel is static for a few bit durations and hence the fading amplitudes do not change within that duration.

By noting that $E[X] = \frac{N_s}{N_B}$ and $E[X^2] = \frac{N_s}{N_B}\left(\frac{N_s}{N_B} - \frac{1}{N_B} + 1\right)$ [18], the mean of Ψ can be given by:

$$\begin{aligned} \mu_{mai} &= \sum_{k=2}^{K} E[Z_{MAI}^{(k)}] \\ &= \frac{m_\psi}{N_B}(m_\Delta)\sum_{k=2}^{K} E_k \sum_{l=1}^{L_c} W_l^2 \sum_{n=1}^{L}(\beta_n^{(k)})^2 \end{aligned} \tag{17}$$

where $m_\psi = \frac{1}{T_c}\int_0^{T_c}\hat{R}_\psi^2(\alpha)d\alpha = \frac{1}{T_c}\int_0^{T_c}R_\psi^2(\alpha)d\alpha$ and $m_\Delta = \frac{N_B(\Delta+1)-1}{N_B-1}$. Next, the standard deviation of Ψ is given as:

$$\begin{aligned} \sigma_{mai} &= \left\{\sum_{k=2}^{K} E[(Z_{MAI}^{(k)})^2] - E[Z_{MAI}^{(k)}]^2\right\}^{(1/2)} \\ &= \left\{\frac{1}{N_s^2}\sum_{k=2}^{K} E_k^2\left[\sum_{l=1}^{L_c}\left(W_l^4\frac{3N_s}{4N_B}w_\Delta w_\psi \sum_{n=1}^{L}(\beta_n^{(k)})^4\right.\right.\right. \\ &\quad + \left(\frac{N_s}{N_B}\right)^2 \frac{m_\Delta^2 w_\psi}{2}\sum_{n=1}^{L}\sum_{\substack{n'=1 \\ n'\neq n}}^{L}(\beta_n^{(k)})^2(\beta_{n'}^{(k)})^2 \\ &\quad \left. + \frac{N_s}{N_B}\frac{w_\Delta \hat{w}_\psi}{2}\sum_{n=1}^{L}\sum_{n'=1}^{L}(\beta_n^{(k)})^2(\beta_{n'}^{(k)})^2\right) \\ &\quad + \sum_{l=1}^{L_c}\sum_{\substack{l'=1 \\ l'\neq l}}^{L_c} W_l^2 W_l'^2 \lambda \\ &\quad \left.\left. - \left(\frac{N_s}{N_B}\frac{m_\psi m_\Delta}{2}\sum_{l'=1}^{L_c} W_l^2 \sum_{n=1}^{L}(\beta_n^{(k)})^2\right)^2\right]\right\}^{(1/2)} \end{aligned} \tag{18}$$

where $w_\psi = \frac{1}{T_c}\int_0^{T_c}\hat{R}_\psi^4(\alpha)d\alpha = \frac{1}{T_c}\int_0^{T_c}R_\psi^4(\alpha)d\alpha$, $\hat{w}_\psi = \frac{1}{T_c}\int_0^{T_c}\hat{R}_\psi^2(\alpha)R_\psi^2(\alpha)d\alpha$, and $w_\Delta = m_\Delta(1 - \frac{m_\Delta}{N_B}) + \frac{N_s}{N_B}m_\Delta^2$. Also, considering that signals captured for different paths are assumed independent for $N_s \geq L$ and dependent for $N_s < L$. Therefore, for $N_s \geq L$, $\lambda = (\frac{N_s}{N_B}m_\Delta m_\psi)^2\sum_{n=1}^{L}(\beta_n^{(k)})^2$, whereas for $N_s < L$, $\lambda = \left[(\frac{N_s}{N_B})^2\frac{m_\Delta^2}{2}\right][w_\psi\sum_{n=1}^{L}\sum_{n'=1}^{L}(\beta_n^{(k)})^2(\beta_{n'}^{(k)})^2 + \hat{w}_\psi\sum_{n=1}^{L}(\beta_n^{(k)})^2(\beta_{(n \mod L)+1}^{(k)})^2]$.

Then, the mean of the MI variance Z_{MI} can be described as:

$$\mu_{mi} = E[Z_{MI}] = \frac{m_\Delta}{2N_B}E_1\sum_{l=1}^{L_c} W_l^2 \sum_{n=1}^{L}(\beta_n^{(1)})^2 \tag{19}$$

Finally, the mean of the narrowband interference variance Z_{nrb} can be described as:

$$\mu_{nrb} = E[Z_{nrb}]$$

$$= 2P_{nrb}\frac{N_s m_\Delta}{N_B}\sum_{l=1}^{L_c} W_l^2 \tilde{B}(\epsilon)\tilde{F}(\epsilon) \quad (20)$$

where $\tilde{B}(\epsilon) = \frac{1}{T_c}\int_0^{T_c} B^2(\epsilon)d\epsilon$ and $\tilde{F}(\epsilon) = \frac{1}{T_c}\int_0^{T_c} F^2(\epsilon)d\epsilon$.

6. Numerical Examples

In this section, the theoretical framework developed is applied to analyze the performance of the system, with specific numerical examples. Asynchronous multiple access system is considered. Although the framework can be used for general cases of any pulse waveforms, in this paper, we consider a cosine baseband envelope $p(t) = \cos(2\pi f_{en\_uwb}t)$, thus giving the unit energy UWB pulse as:

$$v(t) = \frac{p(t)\cos(2\pi f_j^{(k)}t)}{\sqrt{\int_{-\infty}^{+\infty} v^2(t)dt}} \quad (21)$$

where f_{en_uwb} is the transmission rate of the UWB data. The partial autocorrelations of $p(t)$ are given by:

$$\hat{R}_\psi(\alpha) = \frac{\sin(2\pi f_{en\_uwb}\alpha)}{2\pi f_{en\_uwb}\alpha} \quad (22)$$

and $R_\psi(\alpha) = \hat{R}_\psi(T_c - \alpha)$. The overlap of the sub-band bandwidth below -10 dB is assumed neglectable. Since we modeled the collision of the frequency bands among users as in (8), there is no need to allocate specific values for $f_j^{(k)}$.

Next, the coexisting narrowband signal is considered to have a cosine baseband envelope $\xi_s(t) = \cos(2\pi f_{en\_nrb}t)$, where f_{en_nrb} is the data transmission rate of the narrowband signal, and generally, $f_{en\_nrb} \ll f_{en\_uwb}$. The cross-correlation between the UWB signal and the narrowband signal at delay ϵ as in (12) can be given by:

$$\begin{aligned} B(\epsilon) = &\frac{\sin(2\pi(f_{en\_uwb} - f_{en\_nrb})T_c)}{4\pi(f_{en\_uwb} - f_{en\_nrb})}\cos(2\pi f_{en\_nrb}\epsilon) \\ &+\frac{\cos(2\pi(f_{en\_uwb} - f_{en\_nrb})T_c) - 1}{4\pi(f_{en\_uwb} - f_{en\_nrb})}\sin(2\pi f_{en\_nrb}\epsilon) \end{aligned} \quad (23)$$

The multipath channel is considered as a static channel with ten paths, β = [0.59 −0.446 0.39 0.33 −0.29 0.21 0.11 −0.17 0.13 0.07] for all chips and all users. By employing Rake receiver with MRC method, combining weights similar to β are applied.

Here we define system parameters signal to noise ratio (SNR) and signal to interference ratio (SIR). SNR can be given by E_b/N_0 with all users having similar bit energies $E_k = E_b, k = 1, 2, ..., K$ and SIR can be given by $E_b/P_{nrb}T_b$.

The numerical examples are presented and discussed corresponding to different perspectives: namely SNR, suppression coefficient, PG, SIR, number of users and different types of narrowband signals.

6.1 BER Performance vs. SNR

Figure 5 shows the BER performance corresponding to different SNR (E_b/N_0) in both situations with and without the presence of narrowband interference. There are a total of K=10 users all with equal bit energies, PG is set to be 75 with (N_s, N_B)=(5,10). The Rake receiver with MRC method selects and combines L_c=1,2,4 and 10 paths. In order to verify the accuracy of the developed SIGA model, the results for Monte Carlo simulations are shown for L_c=1,2 and 4. From Fig. 5 we can see that the approximations of SIGA closely match the simulation results.

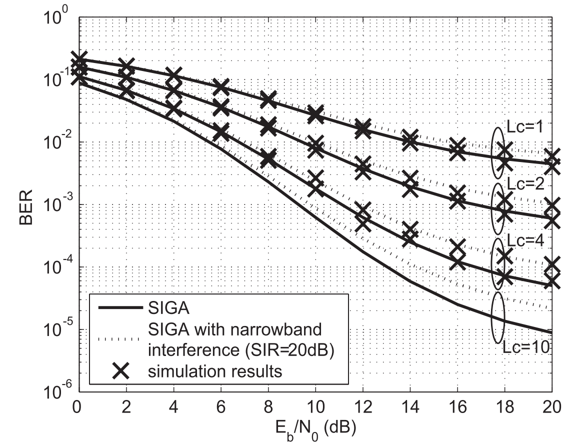

Fig. 5 BER vs. SNR for DS-MB-UWB system in the presence of narrowband interference. Bit energies for all users are equal $E_i = E_b, i = 1, 2, ..., K$. Asynchronous system and MRC method considered. N_s=5, N_B=10, K=10, T_c=4ns, $f_{en\_nrb} = f_{en\_uwb}/80$.

In the presence of narrowband interference, we can see that significant BER degradation takes place, particularly in higher L_c. This is because a portion of the interference is present in every captured path L_c. And by capturing more paths, we also capture more interference. This effect can be reflected in (20) where the narrowband interference component is dependent on parameter L_c.

6.2 BER Performance at Different Sub-Band Power Suppression Levels

Figure 6 presents the relationship between sub-band power suppression level and BER. System parameters such as SNR, PG and L_c are set to 16 dB, 75 and 4 respectively. In the abscissa, suppression coefficient Δ=0 means no suppression moving towards Δ=1 representing full suppression (sub-band elimination).

Firstly, we discuss the results for system A with (N_s, N_B, K)=(5,10,10). We can see that suppressing sub-band power may or may not bring improvement to the BER performance, depending on the strength of the narrowband interference (i.e. SIR). Suppressing the sub-band power is found to be effective generally in the presence of stronger narrowband interference (lower SIR). As SIR becomes higher, suppressing more sub-band power on the other hand, slightly degrades BER performance. This can be explained that in low SIR environment, the main degradation factor is contributed by narrowband interference. Therefore, suppressing the power of the affected sub-band brings significant improvement to the system. However,

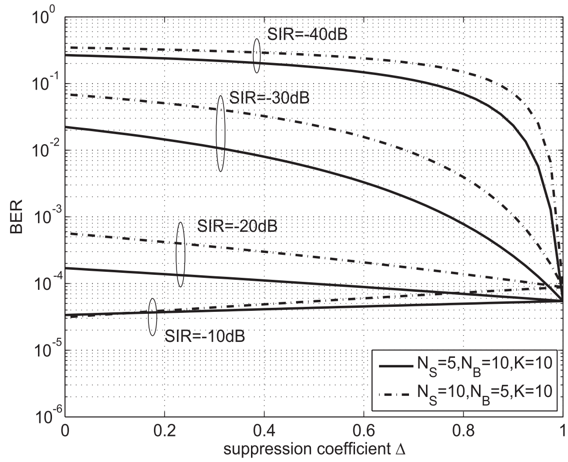

Fig. 6 BER vs. sub-band power suppression coefficient Δ for DS-MB-UWB system in the presence of narrowband interference. SNR=16 dB, PG=75, L_c=4, f_{en_nrb}=f_{en_uwb}/50. System A: (N_s, N_B, K)=(5,10,10) in solid lines, and system B: (N_s, N_B, K)=(10,5,10) in dashed lines.

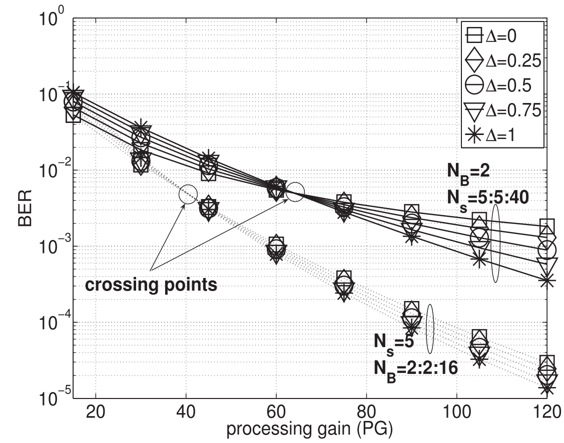

Fig. 7 BER vs. PG=$N_s N_B$ for DS-MB-UWB system. Asynchronous system and Rake receiver with MRC method. SNR=16 dB, SIR=−18 dB, K=10, L_c=4, f_{en_nrb}=f_{en_uwb}/50. System A: (N_s, N_B)=(5:5:40,2) in solid lines, and system B: (N_s, N_B)=(5,2:2:16) in dotted lines.

simultaneously to mitigating narrowband interference, frequency diversity also decreases due to less selection on the affected sub-band while other sub-bands are occupied more frequently, causing MAI and MI to increase. The degradation of frequency diversity is less obvious at low SIR where narrowband interference is dominant, but becomes more noticeable when the suppressed narrowband interference becomes relatively less as compared to the increase of MAI and MI. Therefore, we can see that at higher SIR, suppressing sub-band in the contrary, degrades BER performance.

Secondly, the results of system B with (N_s, N_B, K) =(10,5,10) are discussed. Despite the fact that both systems have the same PG, it is found that system B constantly performs worse than system A, merely because the former has lower N_B. With less number of sub-bands in system B, as sub-band power suppression takes place, the frequency diversity degrades even more rapidly, causing BER to be degraded relatively more severely.

Figure 6 can be divided into two regions: the region where increasing Δ brings BER improvement, and that of the opposite. We know that systems with lower SIR tend to drop into the 'improvement region.' Furthermore, systems with similar PG but lower N_B, will have relatively degraded performance.

In this discussion, we found that mitigating interference by suppressing sub-band power is highly dependent on system parameters such as SIR, number of users, and combination of N_s with N_B. Having different parameters will decide on whether mitigation of narrowband interference will give performance improvement or the contrary.

6.3 BER Performance vs. Processing Gain

Previous results show that PG is a major factor affecting the practicality of sub-band power suppression mitigation-technique. Thus, in this section, Fig. 7 presents the results for PG vs. BER performance corresponding to varying sub-band power suppression. Here, asynchronous multiple access system is assumed, with MRC Rake receiver. The system considers the situation of K=10 users. Here we compare systems with the same PG but different combinations of N_s and N_B.

Firstly, we found that although both systems have similar BER at PG=10, system B outperforms system A collectively as PG increases. This can be explained that in system B, PG is increased by increasing N_B, thus subjected to less 'hit' from narrowband interference when more sub-bands are employed. Additionally, higher N_B also helps in achieving higher frequency diversity (hence less MAI and MI) due to less collision of frequency sub-bands.

Secondly, we can also see that for different values of Δ applied in respective systems, the behaviors may vary. Generally for both systems A and B, at lower PG, system with lower Δ performs better. As PG increases, the contrary will take place, with observable crossing points (PG=55 for system A and PG=40 for system B). And at higher PG, systems with higher Δ is found to outperform those with lower Δ. Here we take note that crossing point is higher in system A than in system B. Also, the performance improvement achievable by employing higher Δ is more pronounced in system A. This is because, when PG is increased by increasing N_s, the frequency diversity is constant, indicating that the system is capable of mitigating more narrowband interference if N_B remains constant while higher Δ is used. Comparatively, the improvement for system B is less significant, even as higher Δ is applied. This is because when PG is increased by increasing N_B (thus increasing also frequency diversity), more sub-bands are made available for frequency hopping, less collision between sub-bands and the narrowband signal takes place, and thus less advantage can be obtained at higher Δ.

This discussion shows that although performance improvement can be achieved by increasing either N_s or N_B, different combinations of the two may bring considerably different results. Choosing the correct combination is essen-

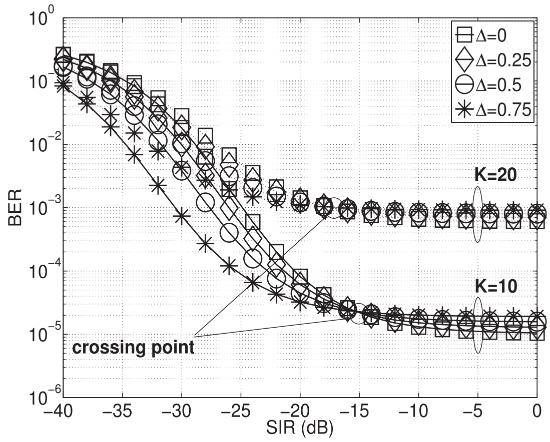

Fig. 8 BER vs. SIR for DS-MB-UWB system. Asynchronous system and Rake receiver with MRC method. SNR=20 dB, N_s=5, N_B=10, L_c=10, f_{en_nrb}=f_{en_uwb}/50.

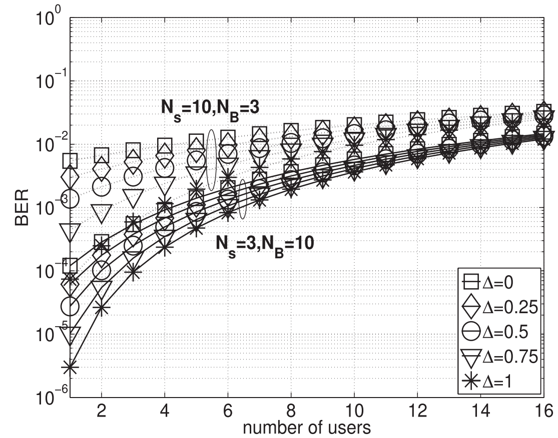

Fig. 9 BER vs. number of users for DS-MB-UWB system. Asynchronous system and Rake receiver with MRC method. SNR=14 dB, SIR=−20 dB, PG=45, L_c=4, f_{en_nrb}=f_{en_uwb}/40.

tial to utilize the interference mitigation capability of sub-band suppression method. The advantage of DS-MB-UWB system employing more number of sub-bands is also highlighted in the discussion.

6.4 BER Performance vs. SIR

The investigation on SIR is essential since SIR is one of the determining factors deciding whether sub-band power suppression brings improvement or degradation to system performance. Figure 8 presents the relationship between SIR and BER performance. Both systems have N_s=5, N_B=10, L_c=10 and SNR=20 dB.

As SIR increases, BER improvement can be observed and this is valid for both systems with K=10 and 20. Particularly, at lower SIR region, applying more sub-band power suppression is found to be more effective in narrowband interference mitigation, thus capable of achieving better BER performance. At higher SIR region, saturation of BER improvement despite increasing SIR is observed, with slight degradation noted at higher Δ values. The reason is that at low SIR environment, the narrowband interference is relatively stronger. Hence, suppressing the affected sub-band power improves BER sufficiently. But in higher SIR environments with weaker narrowband interference, suppressing more sub-band power means degrading more frequency diversity, which results in increasing MAI and MI. Additionally, we have also observed a crossing point taking place between high and low SIR regions. And this crossing point is found to decrease to lower SIR value as K increases.

This section highlights the effectiveness of sub-band power suppression in low SIR environment. Also, when the system has to support more number of users, the dimensions of suppressing sub-band power to mitigate narrowband interference becomes limited.

6.5 BER Performance in Multiple Access Channel

It is known that by applying sub-band power suppression in a multiple access channel, less number of users can be supported at the same BER due to the decrease of frequency diversity. In this section, Fig. 9 presents the number of supported users K vs. BER performance. All users are considered time asynchronous. System parameters such as SNR, SIR and L_c are set to 14 dB, −20 dB and 4, respectively. A narrowband signal is considered to be coexisting with the UWB signal.

As K increases, MAI also increases thus degrading BER. However, we can see that different combinations of N_s and N_B give different BER performance, although PG remains constant. Collectively, systems with higher N_B are found to perform better than those with higher N_s. The superior performance is due to the additional frequency diversity offered by employing higher number of sub-bands. Also, we found that as higher Δ is applied, better performance can be achieved, owing to the mitigation of narrowband interference.

This section shows that sub-band power suppression can be applied to support higher number of users in multiple access channel with the presence of a narrowband interference. Careful choice of combinations of different N_s and N_B can also be used to further enhance BER performance.

6.6 BER Performance vs. Different Narrowband Signals

Up to this section, the analysis are conducted based on constant center frequency and bandwidth of the narrowband interference. This section therefore, further the investigation into the BER performance corresponding to different transmission parameters of the narrowband signal.

In Fig. 10, the relationship between BER performance to narrowband signals with different spectral locations and bandwidths is presented. The abscissa is expressed by $(|f_{sub} - f_{nrb}|)/(W_{sub})$, where 0 means similar f_{sub} and f_{nrb}, and the f_{nrb} gradually moves away from f_{sub} as the value increases. The sub-band bandwidth W_{sub} is designed to be 1 GHz. Half of the affected sub-band power is suppressed

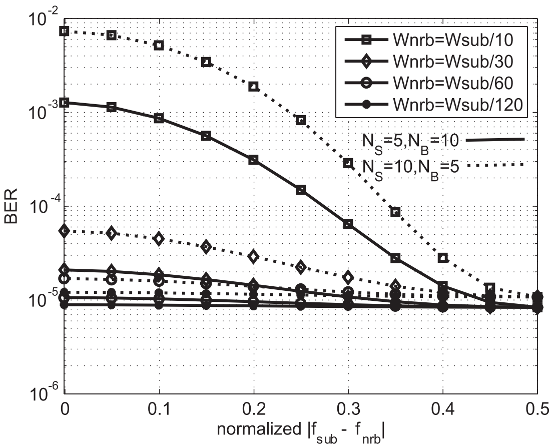

Fig. 10 BER vs. narrowband interference with different spectral locations and bandwidth for DS-MB-UWB system. W_{sub}=1 GHz, Δ=0.5, SNR=14 dB, SIR=−25 dB, K=15, L_c=4. Asynchronous system and Rake receiver with MRC method. W_{nrb}: narrowband signal bandwidth, W_{sub}: UWB sub-band bandwidth, f_{nrb}: narrowband signal center frequency, f_{sub}: UWB sub-band center frequency.

for interference mitigation.

We can see that BER performs the worst when the narrowband signal is exactly located in the middle of the sub-band (i.e. f_{nrb}=f_{sub}). As it goes farther away from the middle, the impact of the interference is found to be less significant. We also found that the wider the bandwidth of the narrowband interference, the more degradation is caused in BER performance. For a narrowband signal with bandwidth 10 times narrower than the UWB sub-band bandwidth, considerably severe impact is observed. The degradation decreases rapidly as W_{nrb} becomes 60 or 120 times narrower. Additionally, with the same PG, UWB system with more number of N_B is more robust to narrowband interference than that with higher N_s.

This discussion shows that BER degradation due to narrowband interference depends greatly on the narrowband signal parameters. Additionally, frequency diversity directly affects the system performance when a narrowband interference is present.

7. Conclusion

This paper has developed the theoretical framework for a DS-MB-UWB system based on SIGA for analysis of performance in the presence of multiple access interference, multipath interference and narrowband interference. The error analysis is compared and validated with Monte Carlo simulation results. We therefore conclude that the framework is capable of accurately characterizing the behavior of the proposed DS-MB-UWB system. Additionally, it is found that the multiband UWB system is able to facilitate mitigation of narrowband interference through sub-band suppression, at the expense of declining frequency diversity. This paper has also provided discussion on the tradeoff between the narrowband interference mitigation and frequency diversity.

Potential future works include extending the investigation to OFDM-UWB system and the comparison with the proposed DS-MB-UWB system.

References

[1] D. Porcino and W. Hirt, "Ultra-wideband radio technology: Potential and challenges ahead," IEEE Commun. Mag., vol.41, no.7, pp.66–74, July 2003.

[2] Federal Communications Commission, "First report and order, revision of part no.15," April 2002.

[3] M.Z. Win and R.A. Scholtz, "Characterization of ultra-wideband wireless indoor channels: A communication-theoretic view," IEEE J. Sel. Areas Commun., vol.20, no.9, pp.1613–1627, Dec. 2002.

[4] European Computer Manufacturers Association, High Rate Ultra Wideband PHY and MAC Standard, ECMA-368, 2nd ed., Dec. 2007.

[5] G.R. Hiertz, Y. Zang, J. Habetha, and H. Sirin, "Multiband OFDM alliance — The next generation of wireless personal area networks," 2005 IEEE/Sarnoff Symposium on Advances in Wired and Wireless Communication, pp.208–214, April 2005.

[6] J.R. Foerster, "The performance of a direct-sequence spread ultra wideband system in the presence of multipath, narrowband interference, and multiuser interference," 2002 IEEE Conference on Ultra Wideband Systems and Technologies 2002, pp.87–91, May 2002.

[7] R.A. Scholtz, "Multiple access with time-hopping impulse modulation," Proc. IEEE MILCOM 1993, vol.2, pp.447–450, Boston, MA, Oct. 1993.

[8] M.Z. Win and R.A. Scholtz, "Ultra-wide bandwidth time-hopping spread-spectrum impulse radio for wireless multiple-access communications," IEEE Trans. Commun., vol.48, no.4, pp.679–691, April 2000.

[9] B. Hu and N.C. Beaulieu, "Accurate performance evaluation of time-hopping and direct-sequence UWB systems in multi-user interference," IEEE Trans. Commun., vol.53, no.6, pp.1053–1062, June 2005.

[10] B. Hu and N.C. Beaulieu, "Accurate evaluation of multiple-access performance in TH-PPM and TH-BPSK UWB systems," IEEE Trans. Commun., vol.52, no.10, pp.1758–1766, Oct. 2004.

[11] S. Gezici, H. Kobayashi, H.V. Poor, and A.F. Molisch, "Performance evaluation of impulse radio UWB systems with pulse-based polarity randomization," IEEE Trans. Signal Process., vol.53, no.7, pp.2537–2549, July 2005.

[12] J.M. Holtzman, "A simple, accurate method to calculate spread spectrum multi-access error probabilities," IEEE Trans. Commun., vol.40, no.3, pp.461–464, March 1992.

[13] Y.C. Yoon, "A simple and accurate method of probability of bit error analysis for asynchronous band-limited DS-CDMA system," IEEE Trans. Commun., vol.50, no.4, pp.656–663, April 2002.

[14] M.A. Rahman, S. Sasaki, J. Zhou, and H. Kikuchi, "Simple-to-evaluate error probabilities for impulse radio UWB multiple access systems with pulse-based polarity randomization," IEEE Commun. Lett., vol.9, no.9, pp.772–774, Sept. 2005.

[15] M.A. Rahman, S. Sasaki, and H. Kikuchi, "Error analysis for Ultra-Wideband DS- and Hybrid DS/TH-CDMA with arbitrary Chip-Duty," IEICE Trans. Fundamentals, vol.E89-A, no.6, pp.1668–1679, June 2006.

[16] K. Siwiak and D. McKeown, Ultra-Wideband Radio Technology, John Wiley and Sons Ltd., West Sussex, England, 2004.

[17] J.G Proakis, Digital Communications, 4th ed., McGraw Hill, New York, 2001.

[18] A. Papoulis and S.U. Pillai, Probability, Random Variables and Stochastic Processes, 4th ed., Tata McGraw-Hill, New Delhi, 2002.

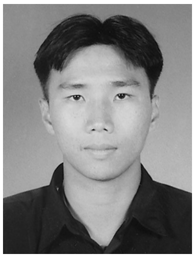

Chin-Sean Sum received his Bachelor's degree in Electrical Engineering (EE) in May 2000 from University Technology Malaysia (UTM), Johor, Malaysia. He then continued his research in sub-millimeter wave systems and received his Master's degree in July 2002 from the same university. From April 2003, he was attached with Niigata University, Niigata, Japan as a Japanese Government (Monbukagakusho) scholar, where later in October 2003 he entered the Department of Electrical and Electronic Engineering as a research student. In April 2004, he started his doctoral course in the same university, focusing on ultra-wideband systems and graduated in March 2007. In June 2007, he joined the National Institute of Information and Communications Technology (NICT), Japan as an expert researcher. In NICT, he joined the Ubiquitous Mobile Communications Group (UMCG) and involved actively in the IEEE 802.15.3c (TG3c) standardization activities of millimeter-wave alternative PHY for wireless personal area network (WPAN). He is currently serving as the TG3c workgroup secretary and the assistant editor for the TG3c draft standard. The team for TG3c standardization received the Best Performance Award of NICT in the year 2007. His research interests are physical and medium access control design for millimeter-wave systems, cross-layer optimization, intersystem coexistence and ultra wideband communication systems. He is a member of IEEE.

Mohammad Azizur Rahman received his Bachelor's degree from Bangladesh University of Engineering and Technology (BUET), Dhaka, Bangladesh in August 2001 and Master's and Ph.D. degrees from Niigata University, Niigata, Japan in March 2005 and 2008 respectively all in Electrical and Electronic Engineering (EEE). From August 2001 to March 2002 he served as a Lecturer in the Department of EEE of BUET. From April 2002 through March 2008, he was attached with Niigata University, Niigata, Japan as a Japanese Government scholar. From October 2007 to March 2008, he was an intern at National Institute of Information and Communications Technology (NICT), Yokosuka, Japan where is presently working as an expert researcher focusing on 60 GHz millimeter wave project. Dr. Rahman was a recipient of *2005 Japan Telecommunication Advancement Foundation (TAF) Technology Award for Students* for outstanding Master's degree thesis. His research interests include wideband communications, CDMA and other multiple access systems, fading channels, diversity receivers etc. He is a member of the IEEE.

Shigenobu Sasaki received B.E., M.E. and Ph.D. degrees from Nagaoka University of Technology, Nagaoka, Japan, in 1987, 1989 and 1993, respectively. Since 1992, he has been with Niigata University, where he is now an Associate Professor in the Department of Electrical and Electronic Engineering. From 1999 to 2000, he was a visiting scholar at the Department of Electrical and Computer Engineering, University of California, San Diego. From 2003 to 2006, he was with the UWB technology institute, National Institute of Information and Communication Technology (NICT) as an expert researcher. His research interests are in the area of digital communications with special emphasis on spread spectrum communication systems, ultra-wideband communication systems, cognitive radio technology and wireless communications. He is a member of IEEE and SITA.

Hiroshi Harada is the director of the Ubiquitous Mobile Communication Group at National Institute of Information and Communications Technology (NICT) and is also the director at NICT's Singapore Wireless Communication Laboratory. He joined the Communications Research Laboratory, Ministry of Posts and Communications, in 1995 (currently NICT). Since 1995, he has researched Software Defined Radio (SDR), Cognitive Radio, Dynamic Spectrum Access Network, and broadband wireless access systems on the microwave and millimeter-wave band. He also has joined many standardization committees especially IEEE 802.15.3c, IEEE 1900.4, IEEE1900.6. He serves currently on the board of directors of SDR Forum and the chair of IEEE SCC41(IEEE P1900) and the vice chair of IEEE P1900.4. He moreover was the chair of the IEICE Technical Committee on Software Radio (TCSR) in 2005–2007. He also is involved in many other activities. He is currently a visiting professor of the University of Electro-Communications, Tokyo, Japan, and is the author of Simulation and Software Radio for Mobile Communications (Artech House, 2002).

Shuzo Kato received his Ph.D. degree in electrical and communications engineering from Tohoku University, Sendai Japan in 1977. From 1977 to 1995, he worked at NTT (Nippon Telegraph and Telephone) Research Laboratories in Japan, specializing personal and satellite communications systems R&D. These include core technology developments for TDMA equipment, modems, and forward error correction schemes in addition to ASIC implementations of PHS (Personal Handy Phone) handsets and many satellite communication terminals. He has managed to develop 39 kinds of ASICs so far without re-spins including the world first TDMA chip set in 1986, the world fastest Viterbi decoder chip in 1987 and 1993, lowest power consumption ADPCM codec (500 μW) in 1994, best receiver sensitivity (6 dB improvement) and the world first 2 V operating CMOS SOC PHS baseband chip (deploying first coherent demodulator for 384 kb/s mobile terminals) and many others. He founded Pacific Communications Research Corp. focusing on ASIC, SW and system design for PCS In 1995, at the same time he served as Senior Executive Vice President, and later as President of Uniden Corporation. From January 1999 to July 2001, he served as Executive Vice President, Mitsubishi Wireless Communications Inc (MWCI) in USA, as well as President, Mobile Communications Technology Center of MWCI in San Diego, CA responsible for mobile phone technology development up to real/sellable and high yield products with all certificates (FCC, CTIA and inter-operability). From 2002 to 2005, he served as Executive Vice President of Teradyne Japan responsible for P/L, Engineering, Production and Global Marketing as well as President and CEO of Omni Wireless Inc., in California, USA. He currently is Professor, Research Institute of Electrical Communications, Tohoku University, Japan, Program Coordinator, Ubiquitous Mobile Communications at NICT (National Institute of Information and Communications Technology) and an Affiliate Faculty Member, Electrical Engineering, University of Hawaii, USA working on wireless communications systems R&D focusing on millimeter wave communications systems. He has been serving as Vice-chair of IEEE802.15.3c Task Group working on millimeter wave systems standardization and Chair of COMPA (Consortium of Millimeter Wave Systems Practical Applications) promoting millimeter wave systems globally. He has published over 200 technical papers, held over 75 patents (including a patent which became DOD (Department of Defense, USA) standard in 1998), co-founded International Symposium on Personal Indoor and Mobile Radio Communications (PIMRC). He is a Fellow of the IEEE and served as an Editor of IEEE Transaction on Communications, Chairman of Satellite and Space Communications Committee, COMSOC IEEE.